Anatase TiO_2 Nanoparticle Coating on Barium Ferrite Using Titanium Bis-Ammonium Lactato Dihydroxide and Its Use as a Magnetic Photocatalyst

Seung-woo Lee,[†] Jack Drwiega,[‡] Chang-Yu Wu,[‡] David Mazyck,[‡] and Wolfgang M. Sigmund*,[†]

Departments of Materials Science and Engineering and Environmental Engineering Sciences, University of Florida, Gainesville, Florida 32611

Received November 18, 2003. Revised Manuscript Received January 28, 2004

Photoactive anatase TiO_2 nanoparticles with a size less than 10 nm were coated on barium ferrite forming complete coverage by the controlled hydrolysis and condensation of titanium bis-ammonium lactato dihydroxide in the presence of polyethyleneimine at a relatively low temperature (95 °C). The as-prepared composite particles (hard magnetic barium ferrite (core)−anatase TiO_2 nanoparticles (shell)) can be utilized as a magnetic photocatalyst, which can be fluidized and recovered by an applied magnetic field enhancing both the separation and mixing efficiency for remediating fluids. The morphology of composite particles was characterized with scanning electron microscopy and transmission electron microscopy. The crystalline structure of TiO_2 was characterized by X-ray diffraction and electron diffraction. Energy-dispersive spectroscopy was utilized for the elemental analysis of the products. The as-prepared TiO_2−barium ferrite composite has higher photocatalytic activities than the TiO_2−barium ferrite composite heat-treated at 500 °C for 1 h. The higher photoactivities of the unheated composite are ascribed to higher specific surface area and preservation of the surface hydroxyl groups on TiO_2.

Introduction

Titanium dioxide (TiO_2) photocatalyst has been widely studied for water and air purification.[1−4] In fact, it is regarded as the best semiconductor photocatalyst for the destruction of organic pollutants in water and air.[5,6] In treating pollutants in water, TiO_2 slurry is the most commonly applied method.[7] Because of its high specific surface area and dispersion, TiO_2 slurry has been demonstrated to be more effective than immobilized TiO_2. However, the use of TiO_2 slurry is still limited mainly due to the difficulty to separate TiO_2 particles from treated water.[8] Recently, iron oxide particles have been coated with TiO_2 to synthesize magnetic photocatalytic particles to recover the photocatalyst particles from the treated water stream by applying an external magnetic field.[9−11] Amal et al.[12,13] reported that they synthesized the magnetic photocatalyst, which was Fe_3O_4 coated with TiO_2 or SiO_2 and TiO_2, with various heat treatments and a couple of different TiO_2 precursors, that is, titanium butoxide and titanium isopropoxide. They demonstrated that the prepared magnetic photocatalysts had comparable photocatalytic activities with respect to anatase TiO_2 that they prepared, which yet need to be improved, compared to Degussa P25 photocatalyst. However, it has been reported that the heat treatment, which is necessary to crystallize the amorphous TiO_2 coating, lowered the specific surface area and the amount of surface hydroxyl groups of TiO_2, eventually decreasing the photoactivity of the magnetic photocatalysts.[14] To minimize the heat treatment step, the modified sol−gel route was adopted to deposit crystalline TiO_2 directly onto the magnetic cores.[14] However, the photoactive TiO_2 layer did not form a uniform coating on the surface of the magnetic cores; rather, they formed patches on the surface when crystalline TiO_2 was directly deposited by the modified sol−gel route. Gao et al.[9] also reported that the heat treatment led to converting the magnetic cores and TiO_2 into an unfavorable Fe_2TiO_5 composite, deteriorating the photocatalytic activity and magnetic properties.

* To whom correspondence should be addressed. Telephone: 1 352 846 3343. Fax: 1 352 846 3355. E-mail: wsigm@mse.ufl.edu.
[†] Department of Materials Science and Engineering.
[‡] Department of Environmental Engineering Sciences.

(1) Hoffmann, M. R.; Martin, S. T.; Choi, W. Y.; Bahnemann, D. W. *Chem. Rev.* **1995**, *95*, 69.
(2) Linsebigler, A. L.; Lu, G. Q.; Yates, J. T. *Chem. Rev.* **1995**, *95*, 735.
(3) Pirkanniemi, K.; Sillanpaa, M. *Chemosphere* **2002**, *48*, 1047.
(4) Bhatkhande, D. S.; Pangarkar, V. G.; Beenackers, A. A. C. M. *J. Chem. Technol. Biotechnol.* **2002**, *77*, 102.
(5) Liu, G. M.; Li, X. Z.; Zhao, J. C.; Hidaka, H.; Serpone, N. *Environ. Sci. Technol.* **2000**, *34*, 3982.
(6) Anpo, M. *Pure Appl. Chem.* **2000**, *72*, 1265.
(7) Crittenden, J. C.; Liu, J. B.; Hand, D. W.; Perram, D. L. *Water Res.* **1997**, *31*, 429.
(8) Sopajaree, K.; Qasim, S. A.; Basak, S.; Rajeshwar, K. *J. Appl. Electrochem.* **1999**, *29*, 1111.
(9) Gao, Y.; Chen, B. H.; Li, H. L.; Ma, Y. X. *Mater. Chem. Phys.* **2003**, *80*, 348.
(10) Chen, F.; Zhao, J. C. *Catal. Lett.* **1999**, *58*, 245.
(11) Beydoun, D.; Amal, R.; Low, G. K. C.; McEvoy, S. *J. Phys. Chem. B* **2000**, *104*, 4387.
(12) Beydoun, D.; Amal, R.; Low, G.; McEvoy, S. *J. Mol. Catal. A* **2002**, *180*, 193.
(13) Beydoun, D.; Amal, R. *Mater. Sci. Eng. B* **2002**, *94*, 71.
(14) Watson, S.; Beydoun, D.; Amal, R. *J. Photochem. Photobiol. A* **2002**, *148*, 303.

10.1021/cm0351902 CCC: $27.50
Published on Web 02/26/2004

In this work, the magnetic photocatalyst was prepared by controlled hydrolysis and condensation of titanium bis-ammonium lactato dihydroxide (TALH) in the presence of polyethyleneimine (PEI). TALH has been used for synthesizing TiO_2 particles[15] and TiO_2 coatings on various substrates.[16−18] The advantages of using TALH as a TiO_2 precursor are that it is a water-soluble precursor, which does not require an alcohol-based solution, and it is stable at ambient temperature in air, which eliminates the need for the use of an inert atmosphere during hydrolysis and condensation procedures. TALH also facilitates the control of hydrolysis and condensation of a TiO_2 precursor due to its stable nature. The present work focused on the synthesis of uniform photoactive crystalline (anatase) TiO_2 layers on the magnetic cores (barium ferrite) using a nonalkoxide TiO_2 precursor in water at relatively low temperature (95 °C). The prepared hard magnetic photocatalysts can not only be recovered but also fluidized by applying an external magnetic field, enhancing both the separation and mixing efficiencies for oxidizing organics in both liquid and air.

Experimental Section

Materials. TALH ($[CH_3CH(O^•)CO_2NH_4]_2Ti(OH)_2$, 50 wt % aqueous solution) from Aldrich Chemicals was used as the TiO_2 precursor without any further purification. Barium ferrite ($BaFe_{12}O_{19}$) from Arnold Engineering and PEI (M_w = 1800) from Alfa Aesar were used in this study. Deionized water (18.2 MΩ•cm, Barnstead "E-Pure") was used in all the experiments. Degussa P25 photocatalyst was supplied by Degussa Corporation. HCl (0.1 N) aqueous solution was purchased from Aldrich.

Preparation of Samples. Two hundred milligrams of barium ferrite particles were dispersed in 150 mL of 1 vol % PEI aqueous solution and sonicated for 5 min in an ultrasonic cleaning bath. After sonication, the PEI aqueous solution was decanted, leaving only PEI adsorbed on barium ferrite particles (PEI−barium ferrite). PEI−barium ferrite, 150 mL of deionized water, and 2 mL of TALH were placed in a 250-mL flask and the pH of the solution was adjusted to 5.5, employing a 0.1 N HCl aqueous solution. The prepared solution was magnetically stirred for 30 min at room temperature and then heated to 95 °C at a rate of 1 °C/min where it stayed for the next 22 h. The prepared sample was recovered from the solution by magnetic separation and washed with deionized water and ethanol. The wet sample was then dried in an oven at 60 °C for 2 days. Half of the dried sample was taken and heat-treated in a furnace at 500 °C for 1 h.

Characterization. The sample images were taken with a transmission electron microscope (TEM, JEOL 200CX) and a high-resolution TEM (HRTEM, JEOL 2010F). A HRTEM was also used to obtain the selected area diffraction patterns. The elemental analysis was conducted using an energy-dispersive X-ray spectroscope (Oxford). X-ray diffraction (XRD) patterns of the powder samples were recorded with a Philips APD 3720 diffractometer. For the compositional analysis, 50 mg of the sample was digested in 100 mL of the sulfuric acid and the analysis was carried out with an inductively coupled plasma (ICP) spectroscope (Perkin-Elmer Plasma 3200). The specific surface area was measured using a BET analyzer (Quantachrome Nova 1200). Zeta potential was measured with a Zeta Reader Mark 21.

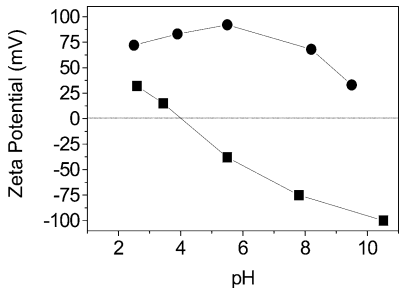

Figure 1. Zeta potential of (■) barium ferrite particles and (●) PEI (M_w = 1800)-adsorbed barium ferrite particles in deionized water as a function of pH.

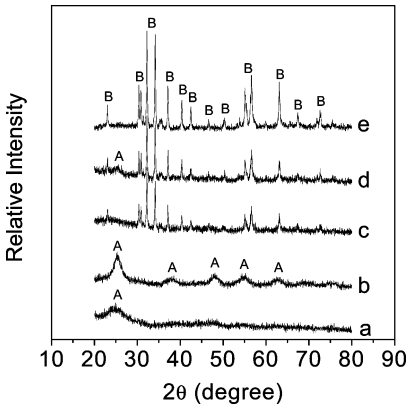

Figure 2. XRD patterns of (a) free TiO_2 nanoparticles, (b) free TiO_2 nanoparticles heat-treated at 500 °C for 1 h, (c) TiO_2−barium ferrite composite, (d) TiO_2−barium ferrite composite heat-treated at 500 °C for 1 h, and (e) uncoated barium ferrite particles. A = anatase. B = barium ferrite.

Photocatalytic Degradation of Procion Red MX-5B. Photodegradation of Procion Red MX-5B (Procion) was conducted in a 100-mL Pyrex glass vessel with magnetic stirring. The illumination sources were four 12-in. 8-W UV bulbs (UVP Inc.) with a wavelength of 365 nm. Aqueous solutions of Procion (50 mL, 10 mg/L) and photocatalyst particles (30 mg of the composite particles, 2.2 mg of TiO_2 particles or Degussa P25, the same amount of TiO_2 was used in all experiments) were placed in a Pyrex vessel. At given intervals of UV illumination, a specimen of the suspension was collected and analyzed by UV−vis spectroscopy using a Perkin-Elmer Lambda 800 spectrophotometer.

Results and Discussion

TiO_2 Coating on Barium Ferrite. In Figure 1, the measured zeta potential of barium ferrite and PEI-adsorbed barium ferrite in deionized water is plotted as a function of pH. PEI adsorption on barium ferrite leads to significant charge reversal. As the pH is lowered from pH 10, the zeta potential of PEI-adsorbed barium ferrite particles increases and the highest value of zeta potential is measured at pH 5.5, reversing the charge from −38 mV to +92 mV. As the pH is lowered again from pH 5.5, the zeta potential decreases. This behavior can be explained from the adsorption and electrokinetic properties of PEI. As the pH is lowered from pH 10, the protonation degree of PEI increases, enhancing zeta potential, whereas the adsorbed amount of PEI decreases due to the electrostatic repulsion between the PEI segments, leading to reduction in zeta potential. Adsorption and electrokinetic properties of PEI are well-described elsewhere.[19]

(15) Mockel, H.; Giersig, M.; Willig, F. *J. Mater. Chem.* **1999**, *9*, 3051.
(16) Caruso, F.; Shi, X. Y.; Caruso, R. A.; Susha, A. *Adv. Mater.* **2001**, *13*, 740.
(17) Hanprasopwattana, A.; Rieker, T.; Sault, A. G.; Datye, A. K. *Catal. Lett.* **1997**, *45*, 165.
(18) Mayya, K. S.; Gittins, D. I.; Caruso, F. *Chem. Mater.* **2001**, *13*, 3833.

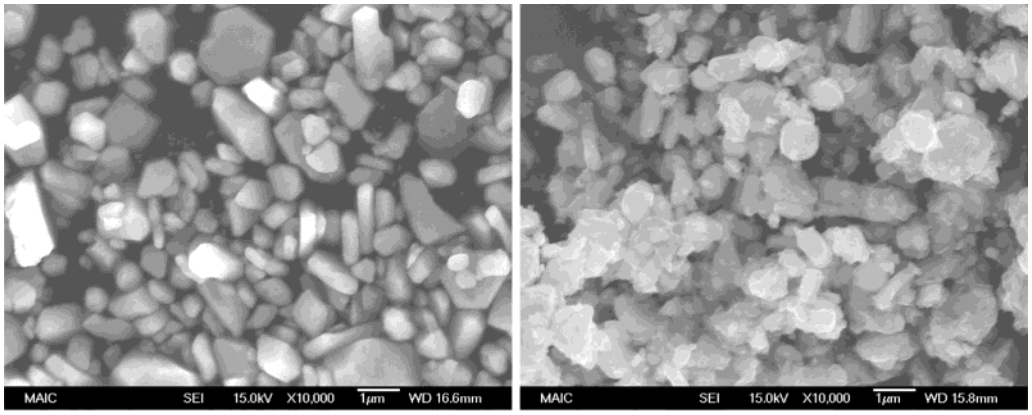

Figure 3. SEM micrographs of (a) uncoated barium ferrite particles and (b) TiO_2−barium ferrite composite particles.

In the TiO_2 coating process, TALH, a doubly negatively charged TiO_2 precursor,[20] is deposited onto the positively charged PEI-adsorbed barium ferrite particles through the electrostatic attraction at room temperature. As stated before, unlike an alkoxide precursor, TALH is relatively stable at ambient temperature in water. Therefore, it is easier to control its hydrolysis and condensation. Another advantage of using TALH as a TiO_2 precursor is that hydrolyzed TALH can be converted into anatase TiO_2 nanoparticles upon heating around 90−100 °C.[16] With controlled heating, TALH undergoes hydrolysis and condensation in a slow manner onto the surface of the barium ferrite particles. During refluxing at 95 °C, hydrolyzed TALH is converted into a TiO_2 network comprised of anatase TiO_2 nanoparticles. TiO_2 loading wt % of the prepared composite is only 7.2% due to the relatively large size of barium ferrite particles. The specific surface area for the as-prepared composite particles (17.9 m^2/g) is enhanced compared with that of uncoated barium ferrite particles (4.1 m^2/g) due to the coating of TiO_2 nanoparticles on barium ferrite. Meanwhile, heat treatment resulted in the growth of TiO_2 particle size, as evidenced by the decrease of specific surface area (11.9 m^2/g). The average particle size of the coated TiO_2, which was measured using a BET analyzer, was 7.6 nm for the as-prepared composite particles and 13.3 nm for the heat-treated composite particles.

XRD patterns of free TiO_2 nanoparticles (free TiO_2 particles from the supernatant after magnetically separating the composite particles), TiO_2−barium ferrite composite particles, and uncoated barium ferrite particles are presented in Figure 2. The peaks from anatase phase of TiO_2 are present in XRD patterns of TiO_2 nanoparticles and TiO_2 nanoparticles heat-treated; however, peaks are very broad and weak due to their nanocrystal size. When the XRD pattern of TiO_2−barium composite particles is compared with that of uncoated barium ferrite particles, the strongest peak of anatase TiO_2 peaks is present at 25.6°; however, the peak is weak and broad since the amount of TiO_2 loading is low and the crystal size of TiO_2 is much smaller than that of barium ferrite.

The SEM images of the as-prepared TiO_2−barium ferrite composite particles and the uncoated barium ferrite particles are given in Figure 3. Different surface morphologies due to TiO_2 coating on the barium ferrite between the composite particles and the uncoated particles are clear in Figure 3. The representative TEM micrographs and selected area diffraction patterns of the prepared samples are presented in Figure 4. Parts (a)−(c) of Figure 4 are taken from the as-prepared sample and (d)−(f) are from the sample heat-treated at 500 °C for 1 h. It is clearly seen that a TiO_2 coating is made on the barium ferrite, forming complete coverage in Figure 4a,d. The thickness of the TiO_2 layer is in the range of 20−40 nm. (b) and (e) of Figure 4 are HRTEM images of the TiO_2 coating region. These lattice-resolving images show that coated TiO_2 nanoparticles are nanocrystalline. The selected area diffraction patterns in (c) and (f) of Figure 4 confirm that the TiO_2 coating is composed of anatase nanocrystalline TiO_2 particles. The selected area diffraction pattern is the ring pattern, which is characteristic of the pattern of nanocrystals. EDS spectrum images taken from the TiO_2−barium ferrite composite is represented in Figure 5. Figure 5a is taken from the core of the TiO_2−barium ferrite composite, showing the presence of Fe, Ba, Ti, and O atoms, whereas Figure 5b is from the TiO_2 coating region, confirming the presence of only Ti and O atoms.

Photocatalytic Performance. The results of photocatalytic performances of the prepared TiO_2−barium ferrite composite particles for photodegradation of Procion Red MX-5B under UV illumination is shown in Figure 6. The photocatalytic performance of a commercial photocatalyst, Degussa P25, and the free TiO_2 particles is also given in the figure for comparison. Both of the as-prepared TiO_2−barium ferrite composite and the heat-treated TiO_2−barium ferrite composite particles are photoactive, as can be seen in Figure 6; however, both of them have lower photocatalytic activities than Degussa P25, which is known as the best photocatalyst commercially available. The higher photoactivity of Degussa P25 can be ascribed to several factors including its larger specific surface area, the 70:30 ratio between anatase and rutile, which tends to promote charge separation, and the existence of surface oxygen vacancies, with their effect on the production of hydroxyl radicals. Nevertheless, it should be recalled

(19) Meszaros, R.; Thompson, L.; Bos, M.; de Groot, P. *Langmuir* **2002**, *18*, 6164.
(20) Shi, X. Y.; Cassagneau, T.; Caruso, F. *Langmuir* **2002**, *18*, 904.

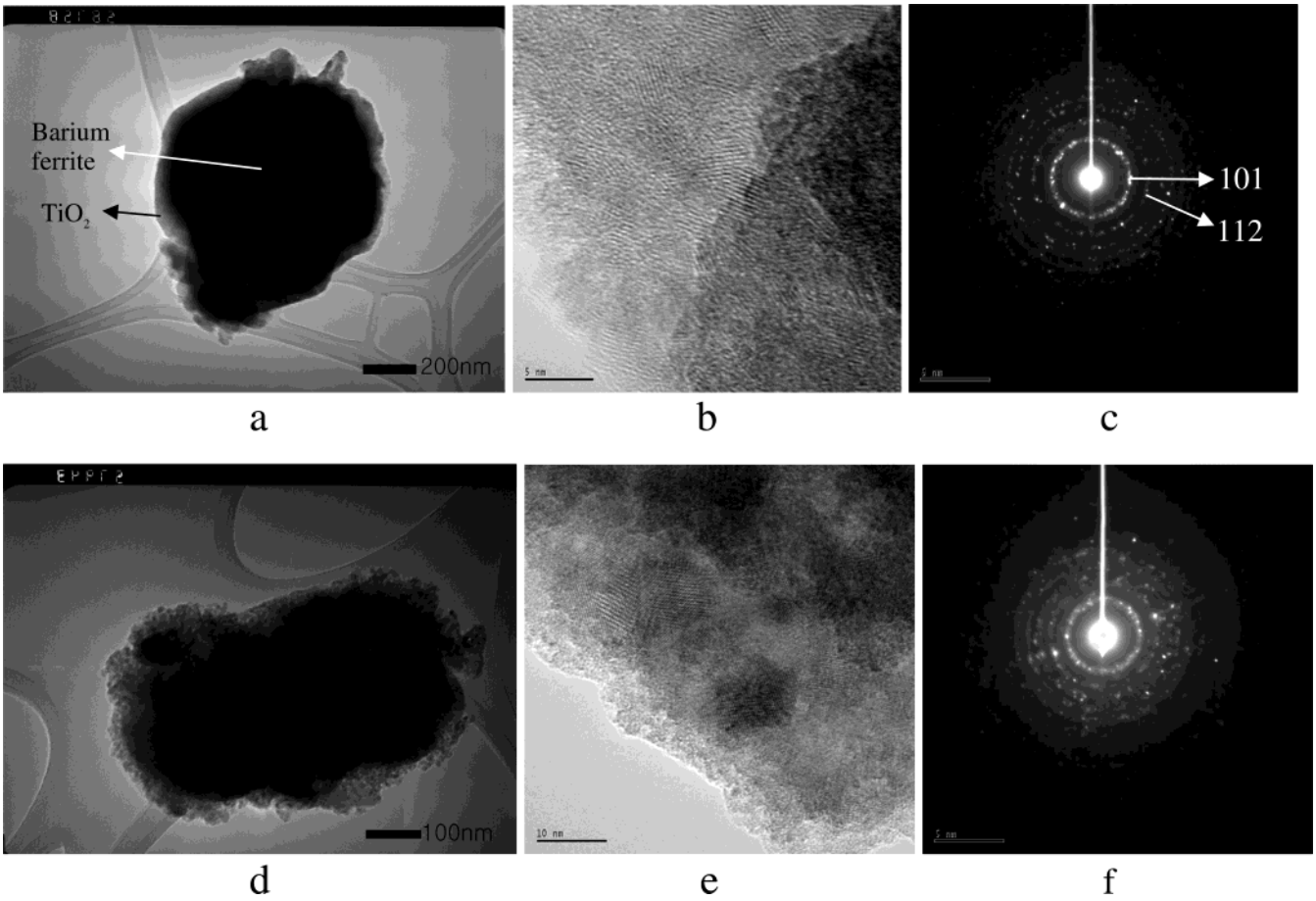

Figure 4. TEM micrographs and selected area diffraction patterns of TiO_2—barium ferrite composite. (a, b, and c) As-prepared sample; (d, e, and f) sample heat-treated at 500 °C for 1 h. (a) TEM image of TiO_2 coating on barium ferrite. (b) HRTEM image of TiO_2 coating and (c) its corresponding diffraction pattern. (d) Heat-treated TiO_2—barium ferrite composite. (e) HRTEM image of TiO_2 coating and (g) its corresponding diffraction pattern.

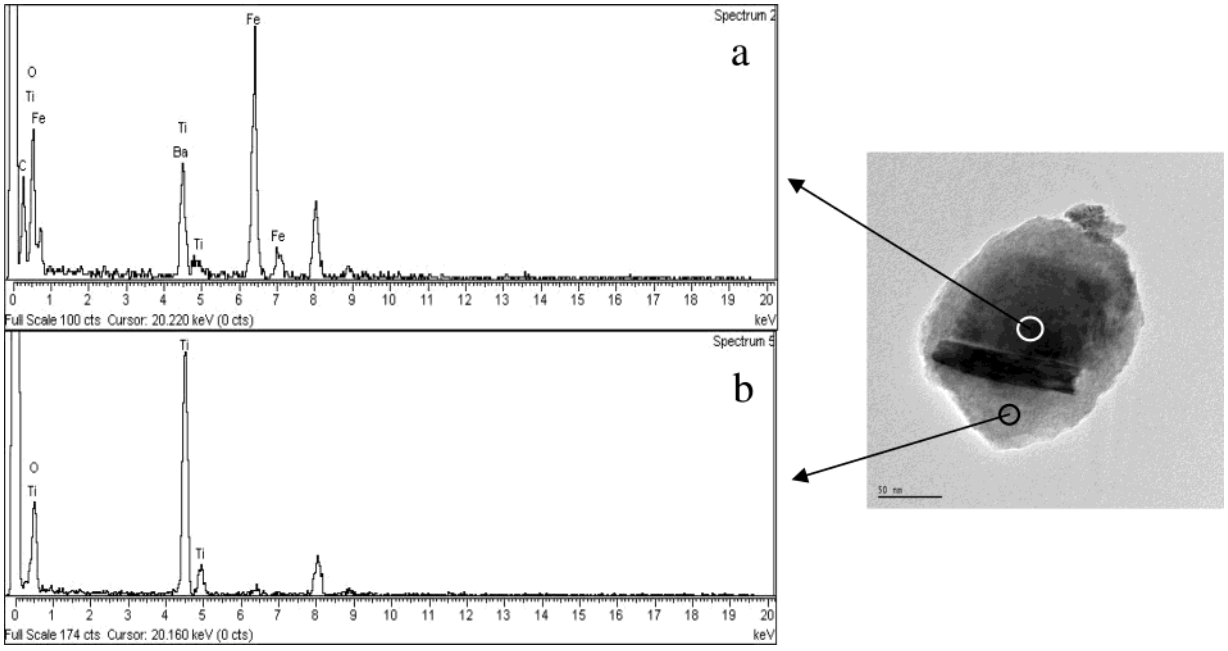

Figure 5. EDS spectrum images of (a) TiO_2—barium ferrite composite particle and (b) TiO_2 coating region of the composite. The unlabeled peaks are adventitious copper.

that the magnetic photocatalyst could be easily recycled while Degussa P25 cannot. Photoactivity of the as-prepared composite is slightly higher than that of the heat-treated composite particles. This is interesting since the as-prepared (unheated) composite particles have less perfect crystallinity than the heat-treated composite particles. A crystallite form of TiO_2, in anatase or rutile phase, is necessary for an efficient pho-

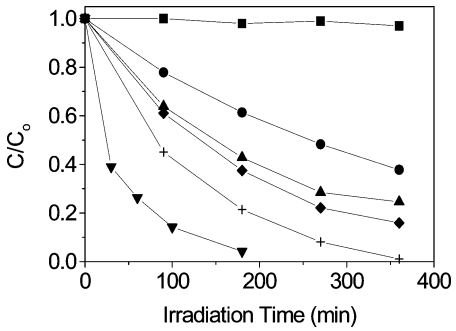

Figure 6. Results of photodegradation of Procion Red MX-5B under UV irradiation with (■) no photocatalyst, (●) TiO_2−barium ferrite composite heat-treated at 500 °C for 1 h, (▲) TiO_2−barium ferrite composite, (◆) free TiO_2 particles heat-treated at 500 °C for 1 h, (+) free TiO_2 particles, and (▼) Degussa P25.

tocatalyst.[21] However, the effects of smaller crystal sizes of TiO_2 nanoparticles in the unheated composite particles compensate for and overcome the effects of the degree of crystallinity. The smaller TiO_2 nanoparticles in the unheated composite lead to higher specific surface area, resulting in higher photocatalytic activities. Another important advantage that the unheated composite has is its better surface property. During the heat treatment of the composite, there is loss of the surface hydroxyl groups on TiO_2, reducing the active sites for the photocatalytic reaction.[22,23] Preserving the surface hydroxyl groups on TiO_2 by minimizing the heat treatment can be one of the reasons for higher photoactivities in the unheated composite particles. The heat treatment can also lead to oxidation of the magnetic core, resulting in loss of magnetic properties.

Conclusion

In this work, TiO_2 has been coated on barium ferrite by the controlled hydrolysis and condensation of titanium bis-ammonium lactato dihydroxide, a water-soluble precursor, from an aqueous system forming complete coverage. It was found that the TiO_2 coating is composed of anatase nanoparticles with a size less than 10 nm. The photocatalytic activities of the prepared TiO_2−barium ferrite composite particles have been tested by the photodegradation of organic dye under UV illumination. The photoactivity of the as-prepared composite was higher than that of the heat-treated composite. The synthesized hard magnetic composite particles can be not only recovered but also fluidized by applying an external magnetic field, enhancing both the separation and mixing efficiencies for treating water and air.

Acknowledgment. This work was financially supported by the U.S. Environmental Protection Agency (EPA)-Science To Achieve Results (STAR) program (Grant R829602).

CM0351902

(21) Ooka, C.; Akita, S.; Ohashi, Y.; Horiuchi, T.; Suzuki, K.; Komai, S.; Yoshida, H.; Hattori, T. *J. Mater. Chem.* **1999**, *9*, 2943.

(22) Sanchez, E.; Lopezm, T.; Gomez Bokhimi, R.; Morales, A. *J. Solid State Chem.* **1996**, *122*, 309.

(23) Gun'Ko, V.; Zarko, V.; Chibowski, E.; Dudnik, V.; Leboda, R.; Zaets, V. *J. Colloid Interface Sci.* **1997**, *188*, 39.